Title
Precision Optogenetic Tool for Selective Single- and Multiple-Cell Ablation in a Live Animal Model System

Permalink
https://escholarship.org/uc/item/4537d0h8

Journal
Cell Chemical Biology, 24(1)

ISSN
2451-9456

Authors
Makhijani, Kalpana
To, Tsz-Leung
Ruiz-González, Rubén
et al.

Publication Date
2017

DOI
10.1016/j.chembiol.2016.12.010

Peer reviewed

Precision Optogenetic Tool for Selective Single- and Multiple-Cell Ablation in a Live Animal Model System

Kalpana Makhijani[1,2,6], **Tsz-Leung To**[1,2,6], **Rubén Ruiz-González**[1,2,3], **Céline Lafaye**[4,5], **Antoine Royant**[4,5], and **Xiaokun Shu**[1,2,7,*]

[1]Department of Pharmaceutical Chemistry, University of California - San Francisco, San Francisco, CA94158, USA

[2]Cardiovascular Research Institute, University of California - San Francisco, San Francisco, CA94158, USA

[3]Institut Químic de Sarrià, Universitat Ramon Llull, Via Augusta 390, Barcelona 08017, Spain

[4]Université Grenoble Alpes, CNRS, CEA, Institut de Biologie Structurale (IBS), Grenoble 38044, France

[5]European Synchrotron Radiation Facility, Grenoble 38043, France

SUMMARY

Cell ablation is a strategy to study cell lineage and function during development. Optogenetic methods are an important cell-ablation approach, and we have previously developed a mini singlet oxygen generator (miniSOG) tool that works in the living *Caenorhabditis elegans*. Here, we use directed evolution to generate miniSOG2, an improved tool for cell ablation via photogenerated reactive oxygen species. We apply miniSOG2 to a far more complex model animal system, *Drosophila melanogaster*, and demonstrate that it can be used to kill a single neuron in a *Drosophila* larva. In addition, miniSOG2 is able to photoablate a small group of cells in one of the larval wing imaginal discs, resulting in an adult with one incomplete and one normal wing. We expect miniSOG2 to be a useful optogenetic tool for precision cell ablation at a desired developmental time point inlive animals, thus openinga new window into cell origin, fate and function, tissue regeneration, and developmental biology.

Graphical Abstract

[*]Correspondence: xiaokun.shu@ucsf.edu.
[6]Co-first author
[7]Lead Contact

AUTHOR CONTRIBUTIONS

X.S. conceived the project. T.-L.T. engineered miniSOG2. T.-L.T. and R.R. performed miniSOG2 characterization. C.L. and A.R. collected spectra of miniSOG2. K.M. created transgenic lines and conducted cell photoablation in *Drosophila*. X.S., K.M., and T.-L.T. wrote the manuscript. All the authors contributed to the final draft.
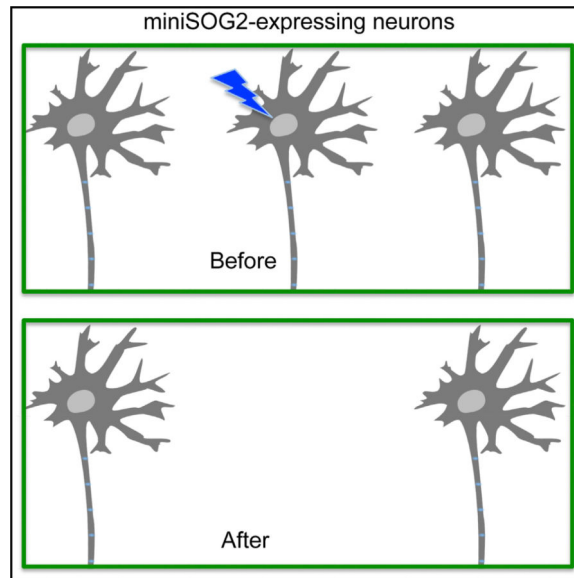
INTRODUCTION

During the development of a multicellular organism, cells differentiate and interact via intracellular and intercellular signaling to generate tissues and organs at the specific time in the appropriate place. It is thus essential to investigate cell origin and fate, cell functions, and cell-cell interactions in order to understand animal development. Cell ablation that selectively removes cells in animals is a powerful technology for developmental biology (Sweeney et al., 2012a). There are four main methods to ablate cells: chemical method, genetic method, laser ablation, and optogenetic method.

The chemical method uses small molecules to ablate cells. For example, hydroxyurea inhibits ribonucleotide reductase, which blocks DNA synthesis and thus kills dividing cells (Sweeney et al., 2012b). Although this method ablates cells during certain developmental events, it has limited specificity. Genetic cell-ablation methods use toxins or apoptosis-inducing genes that are expressed under the control of cell-type-specific promoters (Sweeney et al., 2012a). For example, reconstituted caspase expressed under *mec-18* promoter has been shown to ablate specific neurons in *Caenorhabditis elegans* (Chelur and Chalfie, 2007). The pro-apoptotic gene *reaper* has been demonstrated to kill cells in *Drosophila melanogaster* (White et al., 1996). Toxins such as ricin or diphtheria that inhibit protein translation have been used to eliminate specific neurons in the *Drosophila* embryo (Lin et al., 1995). The M2(H37A) toxic ion channel from the influenza A virus has also been shown to ablate cells in *Xenopus laevis* (Smith et al., 2007) and *Drosophila* (Lam et al., 2010). Bacterial nitroreductase, which reduces the innocuous prodrug metrodinazole to a cytotoxic product, has been shown to ablate cells in the zebrafish using a tissue-specific promoter (Curado et al., 2008). The genetic method often achieves great specificity in cell ablation. But in certain cases expression of death-inducing genes may not be restricted to the desired cell types due to leaky expression of the chosen promoter, and this low-level expression may nonetheless kill cells, leading to off-target ablation (Sweeney et al., 2012a).

The genetic method also suffers from limited spatial and temporal resolution. The ablation method uses intensive light from a laser, which is absorbed within a short time period and is converted into heat, damaging proteins in the cell and resulting in cell death within seconds. A two-photon laser is preferred since it excites the sample with high precision in the z direction, resulting in precise cell ablation. The laser ablation method eliminates cells in animals with the desired spatial pattern at a specific time (Sweeney et al., 2012c). However, dissipation of thermal energy may also lead to damage of neighboring tissues.

The optogenetic method often uses genetically encoded photosensitizers, which produce reactive oxygen species (ROS) upon light excitation, to activate the cell death pathway. It combines advantages of both the genetic and laser ablation methods, and enables cell ablation with single-cell resolution in a specific time. This method also provides a solution to off-target ablation of undesired cell types triggered by leaky expression of toxic genes. The intensity of light used in this method is much lower than that in laser ablation method, which avoids or minimizes non-specific tissue damage. Genetically encoded photo-sensitizers include a red fluorescent KillerRed (Bulina et al., 2006) and a small green fluorescent mini singlet oxygen generator (miniSOG) (Shu et al., 2011). Photoablation of cells using miniSOG has been demonstrated in *C. elegans* (Qi et al., 2012; Xu and Chisholm, 2016), which is an important model organism. *Drosophila* is another important model organism, comprising >1,000 times more cells than *C. elegans*. Because of the genetic tractability and plethora of available genetic tools, *Drosophila* is an attractive model organism for investigation into animal development and disease. However, neither miniSOG (Shu et al., 2011) nor KillerRed (Bulina et al., 2006) (or its monomeric mutant SuperNova [Takemoto et al., 2013]) has been demonstrated in cell photoablation in *Drosophila*. Demonstration of an optogenetic method of cell ablation in *Drosophila* is thus much needed. Instead of using existing photosensitizers, we decided to first improve available photosensitizers in order to maximize success rate in cell photoablation in the transgenic *Drosophila*, which requires more effort and is more time consuming.

RESULTS AND DISCUSSION

Engineering an Efficient Photosensitizer

We used directed evolution to improve the miniSOG for photo-generation of ROS. First, to create a mutant library of miniSOG, we conducted error-prone PCR to introduce random mutations. We used Mutazyme II DNA polymerase that introduces equivalent mutation rates at As and Ts versus Gs and Cs. Second, to screen for improved mutants of miniSOG, we used IFP1.4 as an ROS sensor (Shu et al., 2009). Previously we showed that IFP1.4 reacted with ROS generated from miniSOG (To et al., 2014). Specifically, we fused miniSOG mutants to IFP1.4, which was cloned into a bacterial expression vector pBAD. Expression of this vector led to production of fusion proteins in *E. coli*. We then used a customized bright-blue LED light setting to excite miniSOG mutants by illuminating bacterial colonies grown on agar plates (Figure 1A). The photogenerated ROS reacts with IFP1.4, which leads to decrease of the infrared fluorescence of IFP1.4. We imaged the agar plates in the infrared channel before and after blue-light excitation. We selected the bacterial colonies that displayed the largest infrared fluorescence loss. We conducted DNA shuffling to combine

beneficial mutations from selected mutants (Stemmer, 1994). For each round, we screened about 30,000 mutants or bacterial colonies. After the first round of directed evolution, we improved miniSOG by ~130% as determined by comparing the fluorescence change of the ROS sensor IFP1.4 (Figure 1B). The third round of screening led to a mutant with ~430% improvement. In total, we conducted five rounds of directed evolution, which yielded a mutant with ~7-fold improvement (Figure 1B). We named this mutant miniSOG2. The fluorescence of miniSOG2 is approximately seven times dimmer than miniSOG. Presumably the photon energy is redirected to ROS generation.

We measured the absorbance and fluorescence spectra of miniSOG2 and compared them with miniSOG. The absorbance spectrum revealed significant blueshift of miniSOG2 relative to miniSOG. The visible absorbance peak was blueshifted from 450 nm for miniSOG to 430 nm for miniSOG2 (Figure 1C). The UV absorbance band became narrower with increased absorbance relative to the visible band, in addition to ~20–30 nm blue-shift. The excitation spectra also indicated about 20 nm blueshift for the visible band, and 20–30 nm blueshift for the UV band (Figure 1D). Similar to the absorbance spectra, the UV band also became narrower. In contrast to the absorbance spectra, the fluorescence intensity of the UV band in the excitation spectra decreased relative to that of the visible band, suggesting that the UV band is less efficient in converting absorbed photon energy into fluorescence. Here we focused on the visible band because it is less toxic to cells and animals than the UV band that is within UV-A (315–400 nm), which is generally believed to be phototoxic to cells and animals. The emission spectra of miniSOG2 also showed ~20 nm blueshift (Figure 1E).

Sequence alignment of miniSOG2 and miniSOG revealed seven mutations (Figure 1F). The crystal structure of miniSOG indicated that four of these mutations surround the chromophore flavin mononucleotide (FMN), including R57H, Q44R, G40P, and L84F (Figure 1G). Arginine 57 forms a hydrogen bond with the phosphate group of FMN. Glutamate 44 forms two hydrogen bonds with FMN: one with a ribityl side-chain hydroxyl group, the other with the isoalloxazine group. Both glycine 40 and leucine 84 are positioned close to the FMN isoalloxazine group, with glycine above and leucine below the isoalloxazine group (Figure 1G). The four mutations near the chromophore likely lead to rearrangement of FMN and/or the local structure of the protein near FMN. The large spectroscopic changes of both absorbance and fluorescence spectra would be consistent with such large potential structural changes. The potential conformational changes of FMN and the protein might provide the structural basis for the improved photogeneration efficiency of ROS, the detailed mechanisms of which will require further information including the crystal structure of miniSOG2.

Photoablation of Mammalian Cells by miniSOG2

To demonstrate its application in cell ablation, we expressed miniSOG2 in HEK293 cells. To visualize individual cells by fluorescence, we co-expressed histone 2B (H2B)-EGFP fusion protein, which labels the nucleus. The transfected cells were illuminated with blue LED light (450 nm; ~0.8 W/cm^2) for 1 min. We found that 2 hr after blue-light illumination many cells showed caspase-3 activity (Figures 2A and 2B). As a comparison, the few cells that

expressed SOPP, a recently engineered miniSOG mutant with one single mutation (Westberg et al., 2015), were caspase-3 positive. miniSOG-expressing cells were also rarely caspase-3 positive under the same illumination condition. No caspase-3 activity was detected in the control cells, which only expressed H2B-GFP. Quantitatively, 57% of miniSOG2-expressing cells showed caspase-3 activity, which is significantly higher than SOPP-expressing cells (9%) or miniSOG-expressing cells (11%) (Figure 2C). The morphology of caspase-3-negative cells appeared normal, excluding the possibility of caspase-3-independent types of cell death from these photosensitizers (Figures 2A and S1).

We also found that 4 hr after illumination, for miniSOG2-expressing cells, the percentage of caspase-3-positive cells increased to 86% (Figure 2D). Not surprisingly, the percentage of dying cells also depended on illumination time. Thirty seconds (instead of 60 s) illumination of blue light decreased the caspase-3-positive cells to 21% (Figure 2E). Further decrease of the illumination time to 10 s lowered capase-3-positive cells to 6%. Lastly, we characterized whether the cell killing effect of miniSOG2 is mediated by singlet oxygen. The singlet oxygen quencher, sodium azide (NaN_3), decreased caspase-3-positive cells by 64% (from 81% to 29%) (Figures 2F and 2G). Mannitol, a hydroxyl radical scavenger, showed a smaller inhibition effect with 25% decrease of caspase-3-positive cells (from 81% to 61%).

Optogenetic-Targeted Single-Neuron Ablation in *Drosophila*

Encouraged by the ablation results in cultured cells, we decided to demonstrate miniSOG2 in *Drosophila*. Although several genetically encoded photosensitizers have been developed, none of them has been demonstrated in cell ablation in *Drosophila*. For example, the KillerRed transgenic fly has already been generated (Venken et al., 2011), and its red fluorescence can be observed (Williamson et al., 2012). But it seems that KillerRed has not been successful in photoablation of cells in *Drosophila* (Williamson et al., 2012).

To demonstrate its application in cell ablation in *Drosophila*, we created an upstream activating sequence (UAS)-miniSOG2 T2A Histone 3.3 (H3.3)-EGFP (Table S1) transgenic line and subsequently crossed it with the *ppk*-GAL4 line to promote expression of miniSOG2 in the class IV dendritic arborization (da) neurons (Jan and Jan, 2010; Williams, 2005). T2A is a "self cleaving" peptide widely used in co-expression of multiple genes (Szymczak et al., 2004). Since miniSOG2 is only weakly fluorescent, we used H3.3-EGFP fusion to identify labeled cells. The class IV da neurons cover the body wall of *Drosophila* lava. To visualize neuronal processes, including dendrites and axons, we crossed the above fly with the *ppk*-CD4-tdTomato line (Han et al., 2011). We examined miniSOG2-expressing da neurons of *Drosophila* larvae grown under ambient room light and found that the dendrites appeared to be fragmented (Figure S2). In contrast, for *Drosophila* larvae grown in the dark, the dendrites of miniSOG2-expressing da neurons appeared to be normal, indistinguishable from those of *Drosophila* larvae expressing only CD4-tdTomato (Figure S2). Our data suggest that ambient light induces phototoxicity in miniSOG2-expressing neurons, which is consistent with the previous work using miniSOG in *C. elegans* (Qi et al., 2012). Therefore, to avoid potential phototoxicity from miniSOG2, the *Drosophila* larvae were grown and maintained in the dark.

Illumination of a single neuron with blue light coming from a xenon lamp (excitation filter: 470 ± 20 nm; light intensity: 1.8 W/cm^2) for 3 min around its soma led to loss of tdTomato orange fluorescence in neuronal processes 24 hr after illumination, suggesting ablation of dendrites and axons (Figure 3A). The neighboring neurons that were not exposed to the light remained intact. Furthermore, tdTomato orange fluorescence was little changed 10 min after illumination (Figure 3A), suggesting that loss of the orange fluorescence was not due to photo-bleaching of tdTomato. In the control animals that do not express miniSOG2, tdTomato orange fluorescence in the illuminated neuron was little changed (Figure 3A), suggesting that the neuron remained intact. We also examined neurons 2 hr after blue-light illumination, and found that the illuminated neuron showed swelled, fragmented, and severed dendrites (Figure 3B). Such morphological changes resemble those observed in the class IV da neurons undergoing pruning (Kanamori et al., 2013; Kuo et al., 2006; Lee et al., 2009; Williams et al., 2006). In contrast, the neighboring neurons that were not exposed to blue light showed intact neuronal processes (Figure 3B).

To determine whether ablation of the class IV da neurons results in functional perturbation, we used a blue LED light to illuminate whole animals. The class IV da sensory neurons detect noxious thermal stimuli through their free nerve endings or nociceptors (Soba et al., 2007; Woolf and Ma, 2007; Zhong et al., 2010). We used a previously established assay that provokes locomotory behavior in response to noxious thermal stimuli (Chattopadhyay et al., 2012). Individual third-instar larvae were placed in an 80 μL drop of water on a Petri dish. The Petri dish was then placed on a solid heating block that had already been heated to 95°C. When the temperature of the water drop increased, the larva exhibited stereotyped behaviors including rolling (the larva rolls laterally at least a full 360°). We measured the latency at which the rolling behavior was observed. Then we grouped the larvae into three categories based on the latency: (1) less than 25 s; (2) more than 25 s; (3) no rolling behavior. Freely moving *Drosophila* larvae at 48 hr after egg laying (AEL) were exposed to blue LED light (450 nm; 0.2 W/cm^2) for 6 min. Following illumination, the larvae were incubated in the dark on *Drosophila* cornmeal medium. The larvae were assessed for thermal nociception when they developed to third-instar stage. We compared miniSOG2-expressing larvae with three different control animals including the miniSOG2-expressing *Drosophila* without exposure to light, and *Drosophila* without miniSOG2 either with or without exposure to blue light. The percentage of animals (miniSOG2 + light) that exhibited rolling response within 25 s was significantly lower than that of any one of three control animals including miniSOG2 without light, no min-iSOG2 with light, or no miniSOG2 without light (Figure S3). On the other hand, the percentage of animals (miniSOG2 + light) showing rolling behavior that took more than 25 s appeared to be higher than that of control animals, with a p value of 0.07, approaching the borderline of significance. These data suggest that when illuminated with blue light, many miniSOG2-expressing animals showed perturbed response to noxious thermal stimuli that resulted from ablation of the class IV da sensory neurons.

Photoablation of Wing Imaginal Disc Cells in *Drosophila*

Lastly we investigated whether miniSOG2 can be used in a developmental context. The adult integument of *Drosophila* develops from larval imaginal discs (Figure 4A) (Restrepo et

al., 2014). For example, the adult wings develop from wing imaginal discs. During larval development, the bone morphogenetic protein homolog decapentaplegic (dpp) is expressed in a narrow band of cells anterior to the anteroposterior (A/P) compartment boundary (Figure 4B) (Raftery and Umulis, 2012). The dpp-expressing cells in the wing blade primordium contribute to tissues anterior to the A/P boundary in the adult wing blade (Figure 4C). To express miniSOG2 in the dpp-expressing cells, we crossed UAS-miniSOG2 T2A H3.3-EGFP with the *dpp*-GAL4 line. To avoid potential generation of ROS upon miniSOG2 excitation by ambient room light, we also crossed the fly with *tub*-GAL80[ts]. Gal80[ts] is a temperature-sensitive Gal80, which inhibits Gal4 (McGuire et al., 2003). Thus, this system allows us to express miniSOG2 in the third-instar larvae before photoablation.

We exposed one of the wing imaginal discs of the third-instar larvae to blue light (470 ± 20 nm; 0.5 W/cm^2) for 3 min, with the light restricted within the wing pouch (Figure 4B). In the adult, the wing that was developed from the illuminated wing imaginal disc indicated obvious loss of cells (Figures 4D, 4E, and S4). The cells between longitudinal veins 3 and 4 appeared to be lost; these cells are known to be descendant from the dpp-expressing cells in the wing blade primordium (Figure 4C) (Raftery and Umulis, 2012). On the other hand, the tissues developed from the dpp-non-expressing cells seemed normal including the longitudinal veins 1, 2, and 5, and the posterior cross vein. On the other hand, the wing developed from the wing imaginal disc without being exposed to blue light was normal, including longitudinal and cross veins (Figures 4D, 4F, and S4). For animals expressing miniSOG2 without being exposed to blue light for both wing imaginal discs, both adult wings were normal (Table S2 and Figure S5).

We then conducted experiments for control animals with the same procedure. The control *Drosophila* expressed nuclear GFP under *dpp*-GAL4 and *tub*-GAL80[ts]. Similar to the previous experiment, one of the wing imaginal discs was exposed to blue light for 3 min. Both adult wings were normal (Figure S6), suggesting that the blue light itself was not responsible for the cell loss in the previous experiment. This result confirms that miniSOG2 specifically photoablated the cells in the wing imaginal disc.

In summary, we have significantly improved miniSOG in ROS generation using directed evolution. The improved mutant min-iSOG2 has been demonstrated to induce tissue-specific cell photoablation in the *Drosophila* larvae, including ablation of single sensory neurons and wing imaginal disc cells. Our study is the first successful demonstration of optogenetic cell ablation in *Drosophila* with single-cell resolution. Our work thus shows a powerful technology for studying developmental biology in *Drosophila*. In the future, the miniSOG2-based optogenetic ablation method may be used to ablate subcellular structures such as certain dendrites rather than whole neurons, which can be used to study neurite regeneration as well as cellular response to ROS stress. In addition, miniSOG2 may also be used to photoablate cells and structures in the adult fly. However, such an application is likely to be limited to superficial tissues of the adult animals because of scattering and inefficient penetration of the blue light. In principle, the miniSOG2-based optogenetic cell-ablation method can also be used to other animals such as *C. elegans*, zebrafish, and mice. Our work paves the way to these broader applications, which, however, requires further and detailed studies. For example, the success of potential photoablation of subcellular structures will

depend on how diffusible miniSOG2 and ROS are, which determines how local the photoinduced damage can be, and whether the rest of the cell still behaves normally. Application of miniSOG2 in other animals will require optimization of experimental parameters in the specific animals. For example, for application of miniSOG2 in *C. elegans*, the duration of light exposure may be different from that of *Drosophila*. Furthermore, the previous conditions optimized for miniSOG in *C. elegans* might be different for the miniSOG2-based method because of the modified spectroscopic properties of the latter. Finally, as a technical note, to induce efficient cell photoablation using miniSOG2 the choice of light source is important. Based on our experience, light from a xenon lamp induces efficient cell photoablation with miniSOG2. In contrast, light from scanning lasers is inefficient. It is also recommended to avoid exposing animals to ambient light since it may induce phototoxicity, e.g., dendrite fragmentation as shown in min-iSOG2-expressing neurons in *Drosophila* larvae. In addition, we recommend using a regulated expression system such as GAL80^{ts} to limit duration of miniSOG2 expression in order to further limit potential phototoxicity from miniSOG2. Overall, for future application of the miniSOG2-based optogenetic cell-ablation method in other tissues in *Drosophila* or in other animals, the optimized conditions from our work can be used as a starting point, but specific optimization of experimental conditions is recommended.

SIGNIFICANCE

Our newly developed miniSOG2 enables an optogenetic method for cell ablation in *Drosophila*. We have demonstrated that miniSOG2 can be used to ablate neurons and wing imaginal discs in *Drosophila* larvae using light- and genetic-targeting methods such as the UAS-GAL4 system. Since a large number of recently developed GAL4 lines are available (Jenett et al., 2012; Jory et al., 2012; Manning et al., 2012), miniSOG2 can be used to study the function of many specific types of cells, including neurons. By restricting the illumination area, miniSOG2 allows us to ablate single cells at the desired developmental time point in live animals. The precision of this method is enhanced by the possibilities of genetic targeting, and spatial and temporal control that will make it useful for developmental biology in studying cell origin, fate, and function. It may also be useful in studying tissue regeneration (Worley et al., 2012), cell-cell interactions such as in neuronal circuits, and of the interaction between apoptotic cells and phagocytes.

EXPERIMENTAL PROCEDURES

DNA Constructs

The details of all constructs in this study are listed in Table S1. All plasmid constructs were created by standard molecular biology techniques and confirmed by exhaustively sequencing the cloned fragments. To create the base construct for miniSOG mutagenesis and screening, we fused IFP1.4 (Shu et al., 2009) to the N terminus of the wild-type miniSOG (Shu et al., 2011). A six-aminoacid GSMSGG was inserted between IFP1.4 and miniSOG and the fusion protein was expressed with a C-terminal polyhistidine-tag on a pBAD expression vector (Invitrogen) for expression in *E. coli*. For biliverdin production in *E. coli*, the bacterial heme oxygenase-1 gene codon optimized for *E. coli* was co-expressed using a

ribosomal binding site on the same vector. For mammalian expression and characterization, the miniSOG variants were cloned into the pcDNA3.1 vector (Life Technologies). The miniSOG variants were co-expressed with a fluorescent marker of histone-EGFP, using a *Thosea asigna* virus 2A-cleavage site (T2A). For the histone marker, human histone 2B (H2B) was used for mammalian cell expression. Single-point mutation (i.e., Q102L) was introduced into the original miniSOG on pcDNA3.1 using the QuikChange Lightning Kit (Agilent Technologies), which created SOPP. Finally, for characterization in *Drosophila*, miniSOG2 was cloned into pIHEU vector (gift from Chun Han, Cornell University), which was based on the commonly used pUAST. The construct includes a histone 3.3 (H3.3)-EGFP fluorescent marker to allow identification of cells carrying miniSOG2.

Mutagenesis and Screening

The best-performing miniSOG mutant, miniSOG2, was resulted from five rounds of genetic modifications on the original miniSOG. It was screened from three rounds of random mutagenesis, followed by one round of DNA shuffling and one final round of random mutagenesis. PCR-based random mutagenesis was performed using the Genemorph II Random Mutagenesis Kit (Agilent Technologies). DNA shuffling was performed according to the protocol by Yu et al. (2014). The miniSOG library was cloned in frame at the C terminus of IFP1.4 on the pBAD vector with BamHI and EcoRI. To identify improved mutants, the miniSOG mutant library was expressed in *E. coli* strain TOP10 and grown overnight on Luria-Bertani (LB)-agar plates supplemented with 0.02% (w/v) L-arabinose (Sigma) at 37°C and screened by imaging the colonies on the agar plates using a BioSpectrum Imaging System (UVP) in the IFP channel (excitation, 690 nm; emission, 720 nm). IFP images of the agar plate were taken before and after illumination with a 450 nm blue LED light (Innovations in Optics) at an intensity of ~50 mW/cm^2 for 5 min. The entire agar plate was covered by LED light during the illumination process. When fused to miniSOG, the intensity of IFP decreases upon reaction with ROS generated from photoexcited miniSOG (To et al., 2014). To aid image processing, an image of the agar plate in the minSOG channel (excitation, 475 nm; emission, 535 nm) was acquired before LED illumination. Image process was performed using custom software written in MATLAB (MathWorks). The IFP images before and after LED illumination were aligned by image registration. Putative colonies were identified by thresholding using the pre-illumination IFP image. The difference in IFP intensities before and after LED illumination was computed. For each round of screening, 20–30 Petri dishes (100 mm in diameter) were illuminated and imaged, which totaled more than 30,000 colonies. About five colonies with the largest decrease in IFP intensities were picked, re-plated, and verified with LED illumination. The best mutant (largest decrease in IFP intensity upon illumination) was used as the template for the subsequent round of random mutagenesis. After three rounds of random mutagenesis, the ten best mutants were shuffled. The best mutant from the shuffled library was used as template for the next (and final) round of random mutagenesis.

Protein Purification and Characterization

MiniSOG and miniSOG2 were expressed as 6x His-tagged recombinant protein in *E. coli* CodonPlus (DE3)-RIL Cells (Stratagene). One liter of LB broth medium containing 1 mM ampicillin was inoculated with 10 mL of an overnight culture at 37°C. At an OD$_{600}$ of

approximately 0.6, expression of miniSOG or miniSOG2 was induced by the addition of 0.02% of arabinose, and cells were grown for an additional 24 hr at 37°C. Cells were pelleted by centrifugation ($4,000 \times g$, 4°C, 30 min), resuspended in buffer A (20mMTris-HCl [pH 8.0] and 500 mM NaCl), complemented with complete protease inhibitors-EDTA (Roche) and disrupted using a sonicator. The soluble fraction was recovered by centrifugation ($40,000 \times g$, 4°C, 30 min) and loaded on a 5 mL Ni-NTA Superflow Column (QIAGEN) pre-equilibrated with buffer A. The His-tagged protein was eluted with 150 mM imidazole in buffer A.

Confocal Imaging of Mammalian Cells

For characterization of the miniSOG variants in cultured mammalian cells, transfected HEK293T/17 were imaged in 35 mm glass-bottom microwell dishes on a Nikon Eclipse Ti Inverted Microscope equipped with a CSU-W1 confocal scanner unit (Yokogawa), a digital ORCA-Flash4.0 CMOS camera (Hamamatsu), an ASI MS-2000 XYZ Automated Stage (Applied Scientific Instrumentation) and a Nikon Plan Apo λ 20× air (numerical aperture of 0.75) objective. Laser inputs were provided by an Integrated Laser Engine (Spectral Applied Research) equipped with laser lines (Coherent) 488 nm (6.3 mW) for GFP imaging and 561 nm (3.5 mW) for caspase-3 dye imaging. The confocal scanning unit was equipped with the following emission filters: 525/50 nm for GFP imaging and 610/60 nm for caspase-3 dye imaging.

Characterization in Mammalian Cells

The HEK293T/17 (ATCC CRL-11268) stocks were obtained from ATCC. Cells were passaged in DMEM supplemented with 10% fetal bovine serum, nonessential amino acids, penicillin (100 units/mL), and streptomycin (100 μg/mL). All culture supplies were obtained from the UCSF Cell Culture Facility.

To quantify the efficiency of miniSOG2-mediated cell ablation in mammalian cells, we opted to assay for active caspase-3 levels in ablated cells using the Image-iT LIVE Red Caspase-3 and −7 Detection Kit (Thermo Fisher Scientific). HEK293T/17 cells were transiently transfected with pcDNA3.1 plasmid expressing the miniSOG variant of interest using the calcium phosphate method. Since the caspase-3 dye (FLICA reagent) contains a sulforhodamine group that fluoresces in the red channel, the miniSOG variant was co-expressed with green fluorescent marker (H2B-EGFP) to allow identification of transfected cells. Cells were grown in 35 mm glass-bottom microwell (14 mm) dishes (MatTek Corporation). Transfection was performed when cells were cultured to ~50% confluence. For each transfection, 4.3 μg of plasmid DNA was mixed with 71 μL of $1 \times$ Hank's balanced salt buffer and 4.3 μL of 2.5 M $CaCl_2$. Cells were then incubated at 37°C and 5% CO_2 for 24 hr prior to photoablation.

To perform miniSOG2-mediated photoablation and the subsequent quantification of caspase-3 activity, HEK293T/17 cells expressing miniSOG2 were illuminated with a 450 nm blue LED light (Innovations in Optics) while in growth medium. A LED intensity of ~0.8 W/cm^2 was used for the illumination unless otherwise noted. The entire 35 mm glass-bottom dish was covered by blue light during photoablation. After illumination, cells were returned

to the incubator. One hour before the intended time point for imaging, the FLICA reagent from the Image-iT LIVE Red Caspase-3 and −7 Detection Kit was added at 13 to the cell-culture medium. Cells were incubated for 60 min under existing culture conditions. Afterward, cells were washed twice with the apoptosis wash buffer provided by the detection kit, and imaged in PBS (without fixation) using the confocal microscope described above. To quench ROS production from miniSOG2, 5mM sodium azide or 60mM mannitol was added to the cells prior to photoablation.

For photoablated mammalian cells treated with the FLICA reagent, the fluorescence intensities in the GFP and FLICA channels were measured using the NIS-Elements Advanced Research software (Nikon). In brief, the GFP image was used to identify individual cells using the histone-GFP signal, which can be readily utilized for thresholding and object identification using the built-in ROI tools provided by the NIS-Elements software. The fluorescence intensity of FLICA in the region overlapping with the histone-GFP signal was measured for each cell. Since the fluorescence from the FLICA reagent is evenly distributed within a cell, the average nuclear fluorescence intensity is representative of the entire cell. For each experimental sample, about 500 single cells were measured for GFP and FLICA intensities. The data were exported to MATLAB (MathWorks) for subsequent visualization and analysis. To define the threshold of FLICA intensity for caspase-3-positive cells, we measured the fluorescence of an FLICA-stained sample without miniSOG2. The highest FLICA background intensity observed within a single cell was found to be ~700 counts, after subtracting the camera background noise of 400 counts (Figure 2B). As such, a cutoff of 1,100 counts in FLICA intensity (>1.5 times the maximum value in the negative control population) was used to define the caspase-3-positive population. The fraction of caspase-3-positive cells in Figure 2 is defined as the number of cells with FLICA intensity above the cutoff divided by the total number of histone-GFP-positive cells. The error bars in Figure 2C represent 95% CIs and were obtained by bootstrapping.

Drosophila Strains

The following *Drosophila* lines were used in this study: UAS-CD4-tdGFP (third chromosome insertion) (Han et al., 2011), UAS-nlsGFP (second chromosome insertion, Bloomington Stock Center), *dpp*-GAL4 (second chromosome insertion) (Roy et al., 2011), *ppk*-GAL4 (third chromosome insertion) (Kuo et al., 2005), and *ppk*-CD4-tdTomato (second chromosome insertion) (Han et al., 2011). *w1118* was used as the wild-type strain. Unless noted otherwise, fly crosses were maintained at 25°C. The *Drosophila* transgenic of UAS-min-iSOG2 T2A H3.3-EGFP was generated in this study by using attP insertion on the second chromosome.

Photoablation of Individual Neurons under Fluorescence Microscopy

The genotype of *Drosophila* larvae used in the experiment is: *ppk*-CD4::tdTomato/UAS-miniSOG2 T2A H3.3-GFP; *ppk*-GAL4/+. The genotype of control larvae is: *ppk*-CD4::tdTomato/+; *ppk*-GAL4/+. The age of larvae used is 48–72 hr AEL. The larva was anesthetized with diethyl ether and placed in a drop of 80% glycerol in a glass-bottom imaging dish and oriented in such a way that one of its dorsolateral sides can be imaged. The

sensory neurons were imaged using a Nikon spinning disc confocal with z step size of 1–2 μm. A single miniSOG2-expressing neuron was illuminated using the fluorescein isothiocyanate (FITC) excitation filter (470 ± 20 nm) for 3 min, with light intensity at 1.8W/cm^2. We used a Digital Micromirror Device projector for illumination and created a circular illumination pattern that covers only the soma of a single neuron. Following illumination, the larva was washed in water and saved on *Drosophila* cornmeal medium for observation and imaging of the light-exposed sensory neuron and its neighboring neurons.

Drosophila Behavior Assay for the Function of Class IV da Sensory Neurons

We assessed thermal nociception in *Drosophila* third-instar larvae using the global heat-plate assay (Chattopadhyay et al., 2012). The heat-plate assay was designed to measure thermal nociception in *Drosophila* larvae confronted with a noxious thermal stimulus. Individual third-instar larvae are placed in an 80 μL drop of water on a 60×15 mm Petri dish. The Petri dish is then placed on a solid heating block that is already heated to 95°C. As the temperature of the water drop rises, the larva exhibits stereotyped behaviors including rolling (the larva rolls laterally at least a full 360°). We measure the latencies at which the rolling behavior is observed. Then we group the larvae into three categories based on the latency: (1) less than 25 s; (2) more than 25 s; (3) no rolling behavior.

In brief, we placed the heating block into the heat plate and placed the heat plate on the microscope base. Then we turned on the heat plate to achieve a surface temperature of 95°C. We measured 80 μL of distilled water and placed the water drop in the middle of the polystyrene Petri dish. We then gently placed a clean third-instar larva into the middle of the water drop, and placed the Petri dish containing the water drop and the larva on the solid heating block on the heat plate. We started the timer when the Petri dish was placed on the solid heating block and recorded the time of onset of rolling behavior.

Larvae from the following four experimental conditions were analyzed: (1) wild-type white minus larvae with no illumination of blue LED light (450 nm); (2) UAS-miniSOG2 T2A H3.3-GFP/+; *ppk*-GAL4, UAS-CD4-tdGFP/+ larvae with no blue-light illumination; (3) *ppk*-GAL4, UAS-CD4-tdGFP/+ larvae exposed to the blue light; and (4) UAS-miniSOG2 T2A H3.3-GFP/+; *ppk*-GAL4, UAS-CD4-tdGFP/+ larvae exposed to the blue light. *Drosophila* larvae at 48 hr AEL were exposed to the blue LED light (0.2 W/cm^2) for 6 min. Following illumination, the larvae were incubated in the dark on *Drosophila* cornmeal medium. The larvae were assessed for thermal nociception when they developed to third-instar stage. Using the global heat-plate assay, the time of onset of rolling response when an individual larva was exposed to high temperature (95°C) was recorded. The larvae were grouped into three categories: onset of rolling response in less than or equal to 25 s, more than 25 s, and no roll. The percentage of larvae in each category was determined. Each experiment had 15–30 larvae. Four experimental replicates were analyzed for statistical significance.

Photoablation of *Drosophila* Larval Wing Imaginal Disc

The larvae expressing miniSOG2 were obtained from a cross of *dpp*-GAL4; *tub*-GAL80^{ts} X UAS-miniSOG2 T2A H3.3A EGFP. The control larvae were obtained from a cross of *dpp*-

GAL4; *tub*-GAL80^{ts} X UAS-nlsGFP. The crosses were incubated at 18°C until third-instar larval stage. The *dpp*-GAL4 driven expression of miniSOG2 or nlsGFP was induced by incubating the fly food vial containing the progeny larvae at 30°C for 16–18 hr prior to light exposure. The wandering third-instar larvae expressing miniSOG2 or controls expressing UAS-nlsGFP were washed in distilled water to remove fly food sticking to their body. The larvae were then etherized for 5 min and placed on a glass slide with double-sided sticky tape such that the dorsal side of the larva was on top and faced the coverslip side. A coverslip was placed on top of the larvae with a spacer made of a stack of three to four layers of tape placed on the edges between the glass slide and coverslip. This setup allowed us to observe and locate the wing imaginal discs of the larvae and expose them to blue light. The pouch area of the wing imaginal disc was exposed to a circular area of blue light using the FITC filter for a duration of 3 min. The intensity of the blue light used was 0.5 W/cm^2. It was important that the larva remained immobile during the entire light-exposure period and that neighboring imaginal discs such as leg and haltere imaginal discs that also express miniSOG2 from the *dpp*-GAL4 driver were not exposed to blue light. Following light exposure the larva was gently detached from the sticky tape on the glass slide by placing a drop of water on it and then placed in a fly food vial for incubation until eclosion. The survival of the animal and wing phenotypes were assessed following fly eclosion. The dorsal and ventral sides of etherized adult fly were imaged using a Zeiss Discovery V8 stereomicroscope and EOS Rebel T3i (1.6×SLR) digital camera. The adult wings were dissected and mounted in Euparal oil and bright-field images were acquired using a Leica DMR microscope equipped with SPOT CCD camera and SPOT acquisition software. Larvae expressing miniSOG2 but not exposed to light were included as additional negative controls.

Supplementary Material

Refer to Web version on PubMed Central for supplementary material.

Acknowledgments

REFERENCES

Bulina ME, Chudakov DM, Britanova OV, Yanushevich YG, Staroverov DB, Chepurnykh TV, Merzlyak EM, Shkrob MA, Lukyanov S, Lukyanov KA. A genetically encoded photosensitizer. Nat. Biotechnol. 2006; 24:95–99. [PubMed: 16369538]

Chattopadhyay A, Gilstrap AV, Galko MJ. Local and global methods of assessing thermal nociception in *Drosophila* larvae. J Vis. Exp. 2012:e3837. [PubMed: 22643884]

Chelur DS, Chalfie M. Targeted cell killing by reconstituted caspases. Proc. Natl. Acad. Sci. USA. 2007; 104:2283–2288. [PubMed: 17283333]

Curado S, Stainier DYR, Anderson RM. Nitroreductase-mediated cell/tissue ablation in zebrafish: a spatially and temporally controlled ablation method with applications in developmental and regeneration studies. Nat. Protoc. 2008; 3:948–954. [PubMed: 18536643]

Han C, Jan LY, Jan Y-N. Enhancer-driven membrane markers for analysis of nonautonomous mechanisms reveal neuron-glia interactions in *Drosophila* . Proc. Natl. Acad. Sci. USA. 2011; 108:9673–9678. [PubMed: 21606367]

Jan Y-N, Jan LY. Branching out: mechanisms of dendritic arborization. Nat. Rev. Neurosci. 2010; 11:316–328. [PubMed: 20404840]

Jenett A, Rubin GM, Ngo T-TB, Shepherd D, Murphy C, Dionne H, Pfeiffer BD, Cavallaro A, Hall D, Jeter J, et al. A GAL4-driver line resource for *Drosophila* neurobiology. Cell Rep. 2012; 2:991–1001. [PubMed: 23063364]

Jory A, Estella C, Giorgianni MW, Slattery M, Laverty TR, Rubin GM, Mann RS. A survey of 6,300 genomic fragments for *cis*-regulatory activity in the imaginal discs of *Drosophila melanogaster* . Cell Rep. 2012; 2:1014–1024. [PubMed: 23063361]

Kanamori T, Kanai MI, Dairyo Y, Yasunaga KI, Morikawa RK, Emoto K. Compartmentalized calcium transients trigger dendrite pruning in *Drosophila* sensory neurons. Science. 2013; 340:1475–1478. [PubMed: 23722427]

Kuo CT, Jan LY, Jan Y-N. Dendrite-specific remodeling of *Drosophila* sensory neurons requires matrix metalloproteases, ubiquitin-proteasome, and ecdysone signaling. Proc. Natl. Acad. Sci. USA. 2005; 102:15230–15235. [PubMed: 16210248]

Kuo CT, Zhu S, Younger S, Jan LY, Jan Y-N. Identification of E2/E3 ubiquitinating enzymes and caspase activity regulating *Drosophila* sensory neuron dendrite pruning. Neuron. 2006; 51:283–290. [PubMed: 16880123]

Lam VK, Tokusumi T, Cerabona D, Schulz RA. Specific cell ablation in *Drosophila* using the toxic viral protein M2(H37A). Fly (Austin). 2010; 4:338–343. [PubMed: 20798602]

Lee H-H, Jan LY, Jan Y-N. *Drosophila* IKK-related kinase Ik2 and Katanin p60-like 1 regulate dendrite pruning of sensory neuron during metamorphosis. Proc. Natl. Acad. Sci. USA. 2009; 106:6363–6368. [PubMed: 19329489]

Lin DM, Auld VJ, Goodman CS. Targeted neuronal cell ablation in the *Drosophila* embryo: pathfinding by follower growth cones in the absence of pioneers. Neuron. 1995; 14:707–715. [PubMed: 7718234]

Manning L, Heckscher ES, Purice MD, Roberts J, Bennett AL, Kroll JR, Pollard JL, Strader ME, Lupton JR, Dyukareva AV, et al. A resource for manipulating gene expression and analyzing cis-regulatory modules in the *Drosophila* CNS. Cell Rep. 2012; 2:1002–1013. [PubMed: 23063363]

McGuire SE, Le PT, Osborn AJ, Matsumoto K, Davis RL. Spatiotemporal rescue of memory dysfunction in *Drosophila*. Science. 2003; 302:1765–1768. [PubMed: 14657498]

Qi YB, Garren EJ, Shu X, Tsien RY, Jin Y. Photo-inducible cell ablation in *Caenorhabditis elegans* using the genetically encoded singlet oxygen generating protein miniSOG. Proc. Natl. Acad. Sci. USA. 2012; 109:7499–7504. [PubMed: 22532663]

Raftery LA, Umulis DM. Regulation of BMP activity and range in *Drosophila* wing development. Curr. Opin. Cell Biol. 2012; 24:158–165. [PubMed: 22152945]

Restrepo S, Zartman JJ, Basler K. Coordination of patterning and growth review by the morphogen DPP. Curr. Biol. 2014; 24:R245–R255. [PubMed: 24650915]

Roy S, Hsiung F, Kornberg TB. Specificity of *Drosophila* cytonemes for distinct signaling pathways. Science. 2011; 332:354–358. [PubMed: 21493861]

Shu X, Royant A, Lin MZ, Aguilera TA, Lev-Ram V, Steinbach PA, Tsien RY. Mammalian expression of infrared fluorescent proteins engineered from a bacterial phytochrome. Science. 2009; 324:804–807. [PubMed: 19423828]

Shu X, Lev-Ram V, Deerinck TJ, Qi Y, Ramko EB, Davidson MW, Jin Y, Ellisman MH, Tsien RY. A genetically encoded tag for correlated light and electron microscopy of intact cells, tissues, and organisms. PLoS Biol. 2011; 9:e1001041. [PubMed: 21483721]

Smith SJ, Kotecha S, Towers N, Mohun TJ. Targeted cell-ablation in *Xenopus* embryos using the conditional, toxic viral protein M2(H37A). Dev. Dyn. 2007; 236:2159–2171. [PubMed: 17615576]

Soba P, Zhu S, Emoto K, Younger S, Yang S-J, Yu H-H, Lee T, Jan LY, Jan Y-N. *Drosophila* sensory neurons require Dscam for dendritic self-avoidance and proper dendritic field organization. Neuron. 2007; 54:403–416. [PubMed: 17481394]

Stemmer WP. Rapid evolution of a protein in vitro by DNA shuffling. Nature. 1994; 370:389–391. [PubMed: 8047147]

Sweeney ST, Hidalgo A, de Belle JS, Keshishian H. Genetic systems for functional cell ablation in *Drosophila*. Cold Spring Harb. Protoc. 2012a; 2012:950–956. [PubMed: 22949708]

Sweeney ST, Hidalgo A, de Belle JS, Keshishian H. Hydroxyurea ablation of mushroom bodies in *Drosophila*. Cold Spring Harb. Protoc. 2012b; 2012:231–234. [PubMed: 22301647]

Sweeney ST, Hidalgo A, de Belle JS, Keshishian H. Embryonic cell ablation in *Drosophila* using lasers. Cold Spring Harb. Protoc. 2012c; 2012:691–693. [PubMed: 22661443]

Szymczak AL, Workman CJ, Wang Y, Vignali KM, Dilioglou S, Vanin EF, Vignali DAA. Correction of multi-gene deficiency in vivo using a single "self-cleaving" 2A peptide-based retroviral vector. Nat. Biotechnol. 2004; 22:589–594. [PubMed: 15064769]

Takemoto K, Matsuda T, Sakai N, Fu D, Noda M, Uchiyama S, Kotera I, Arai Y, Horiuchi M, Fukui K, et al. SuperNova, a monomeric photosensitizing fluorescent protein for chromophore-assisted light inactivation. Sci. Rep. 2013; 3:2629. [PubMed: 24043132]

To T-L, Fadul MJ, Shu X. Singlet oxygen triplet energy transfer-based imaging technology for mapping protein-protein proximity in intact cells. Nat. Commun. 2014; 5:4072. [PubMed: 24905026]

Venken KJT, Schulze KL, Haelterman NA, Pan H, He Y, Evans-Holm M, Carlson JW, Levis RW, Spradling AC, Hoskins RA, et al. MiMIC: a highly versatile transposon insertion resource for engineering *Drosophila melanogaster* genes. Nat. Methods. 2011; 8:737–743. [PubMed: 21985007]

Westberg M, Holmegaard L, Pimenta FM, Etzerodt M, Ogilby PR. Rational design of an efficient, genetically encodable, protein-encased singlet oxygen photosensitizer. J. Am. Chem. Soc. 2015; 137:1632–1642. [PubMed: 25575190]

White K, Tahaoglu E, Steller H. Cell killing by the *Drosophila* gene reaper. Science. 1996; 271:805–807. [PubMed: 8628996]

Williams DW. Cellular mechanisms of dendrite pruning in *Drosophila*: insights from in vivo time-lapse of remodeling dendritic arborizing sensory neurons. Development. 2005; 132:3631–3642. [PubMed: 16033801]

Williams DW, Kondo S, Krzyzanowska A, Hiromi Y, Truman JW. Local caspase activity directs engulfment of dendrites during pruning. Nat. Neurosci. 2006; 9:1234–1236. [PubMed: 16980964]

Williamson, WR., Chan, C-C., Hiesinger, PR. In The Making and Un-Making of Neuronal Circuits in *Drosophila* Neuromethods. Vol. 69. Humana Press; 2012. Subcellular resolution imaging in neural circuits; p. 61-89.

Woolf CJ, Ma Q. Nociceptors—noxious stimulus detectors. Neuron. 2007; 55:353–364. [PubMed: 17678850]

Worley MI, Setiawan L, Hariharan IK. Regeneration and transdetermination in *Drosophila* imaginal discs. Annu. Rev. Genet. 2012; 46:289–310. [PubMed: 22934642]

Xu S, Chisholm AD. Highly efficient optogenetic cell ablation in *C. elegans* using membrane-targeted miniSOG. Sci. Rep. 2016; 6:21271. [PubMed: 26861262]

Yu D, Gustafson WC, Han C, Lafaye C, Noirclerc-Savoye M, Ge W-P, Thayer DA, Huang H, Kornberg TB, Royant A, et al. An improved monomeric infrared fluorescent protein for neuronal and tumour brain imaging. Nat. Commun. 2014; 5:3626. [PubMed: 24832154]

Zhong L, Hwang RY, Tracey WD. Pickpocket is a DEG/ENaC protein required for mechanical nociception in *Drosophila* larvae. Curr. Biol. 2010; 20:429–434. [PubMed: 20171104]

Highlights

- An efficient photosensitizer miniSOG2 is engineered using directed evolution

- miniSOG2 enables precision photoablation of single neurons in live *Drosophila*

- miniSOG2 allows optogenetic ablation of cells in wing imaginal disc

In Brief

A genetically encoded photosensitizer is engineered to efficiently generate reactive oxygen species, which activate caspase and cell apoptosis. It enables precision optogenetic ablation of single neurons in live *Drosophila* and can be an important tool for studying developmental biology.
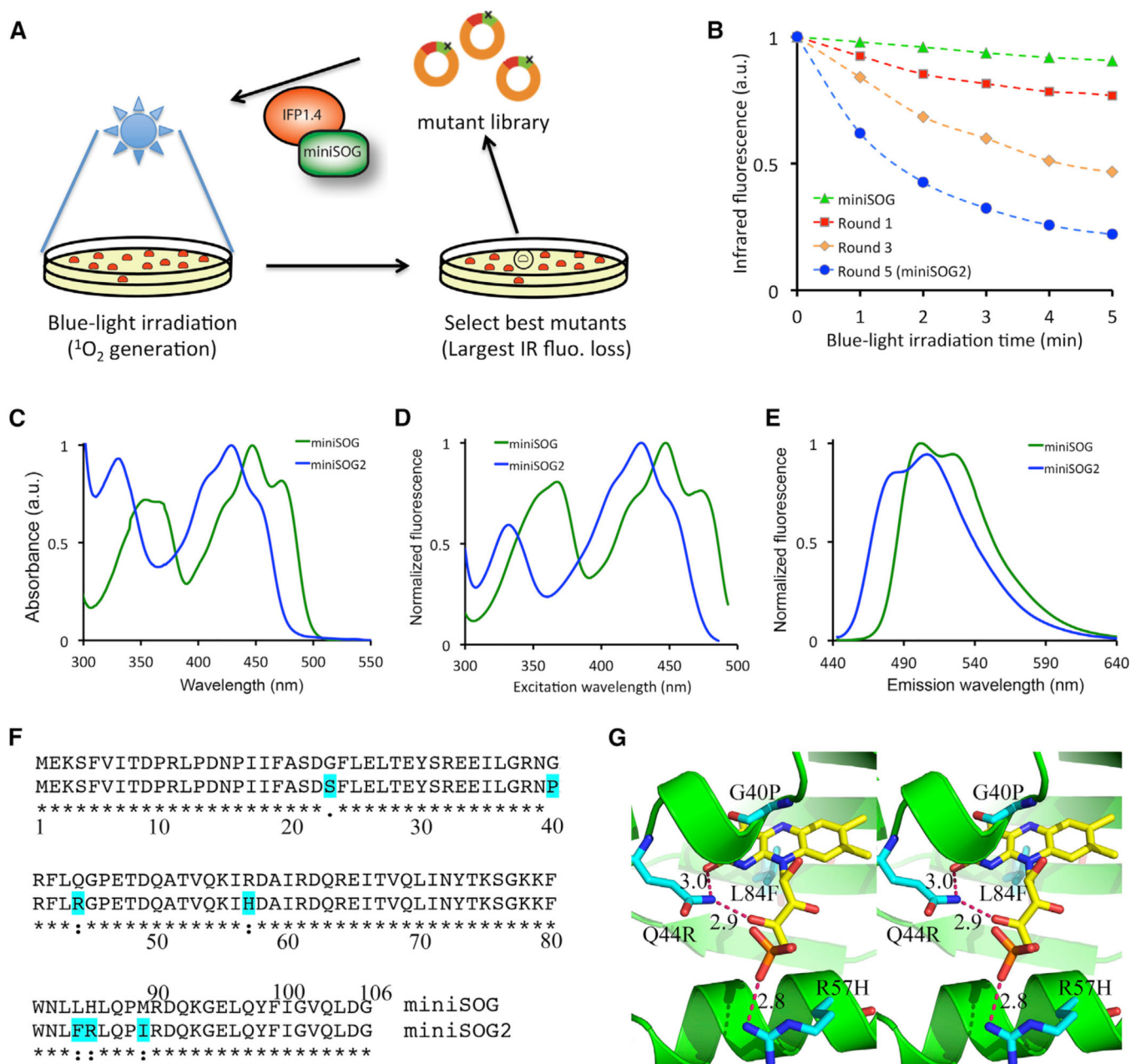
Figure 1. Directed Evolution of a Photosensitizer miniSOG2

(A) Schematic of the strategy used in the directed evolution of miniSOG2. The infrared fluorescent protein 1.4 (IFP 1.4) was used as a sensor. Largest IR fluo. Loss, largest infrared fluorescence loss.

(B) Bleaching of the infrared fluorescence of IFP 1.4 by various miniSOG mutants.

(C–E) Absorbance (C), excitation (D), and emission (E) spectra of miniSOG (green) and miniSOG2 (blue).

(F) Sequence alignment of miniSOG and miniSOG2. The mutated residues are highlighted in cyan.

(G) Stereo image of the crystal structure of miniSOG with four mutated residues that are near the chromophore FMN (yellow). The hydrogen bonds are shown in dashed lines. The numbers represent the length of the hydrogen bonds in nanometer.
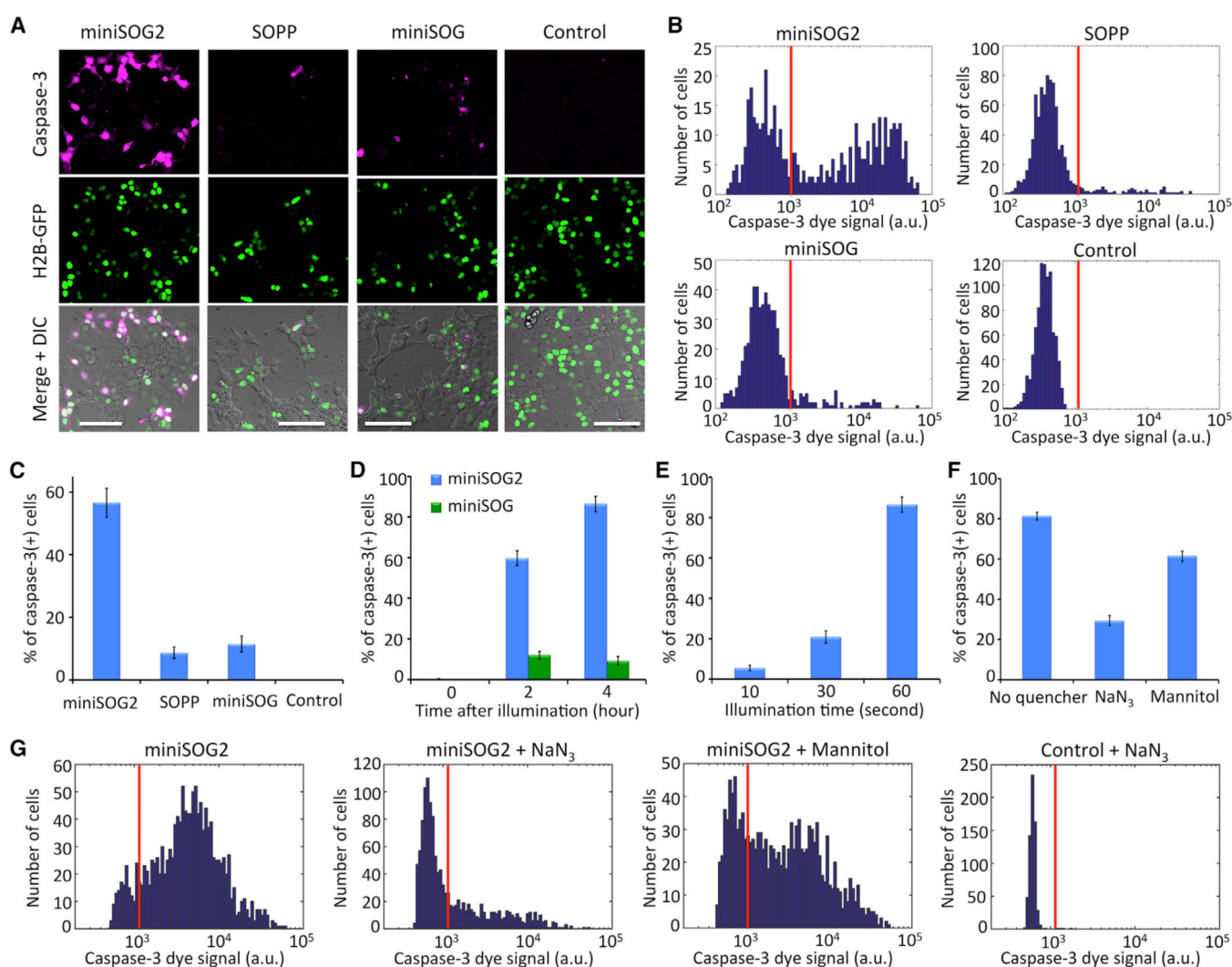
Figure 2. Comparison and Characterization of miniSOG2 in Photoablation of Mammalian Cells

(A) Comparison of miniSOG2 with miniSOG and another mutantSOPP in cell ablation. The cultured HEK293 cells co-expressed histone 2B (H2B)-GFP fusion and miniSOG2 (or miniSOG, SOPP). The control cells expressed H2B–GFP only. Top: red fluorescence from FLICA caspase-3 reagent; middle, green fluorescence from H2B–GFP; bottom, merged images with differential interference contrast (DIC).

(B) Histogram of caspase-3-positive cells after blue-light illumination.

(C) Percentage of caspase-3-positive cells after blue-light illumination. Caspase-3 signal was detected 2 hr after illumination (A), (B), and (C).

(D) Dependence of the percentage of caspase-3-positive cells on the time after blue-light illumination.

(E) Dependence of the percentage of caspase-3-positive cells on the blue-light illumination time. Caspase-3 signal was detected 4 hr after illumination.

(F) Effect of ROS quenchers (the singlet oxygen quencher NaN3, and hydroxyl radical quencher mannitol) on the photoablation of HEK293 cells expressing miniSOG2. The error bars in (C–F) represent 95% confidence intervals by bootstrapping.

(G) Histogram of different ROS quenchers on cell photoablation. Cells were illuminated for 1 min and caspase-3 signal was detected 3 hr after illumination (F) and (G).

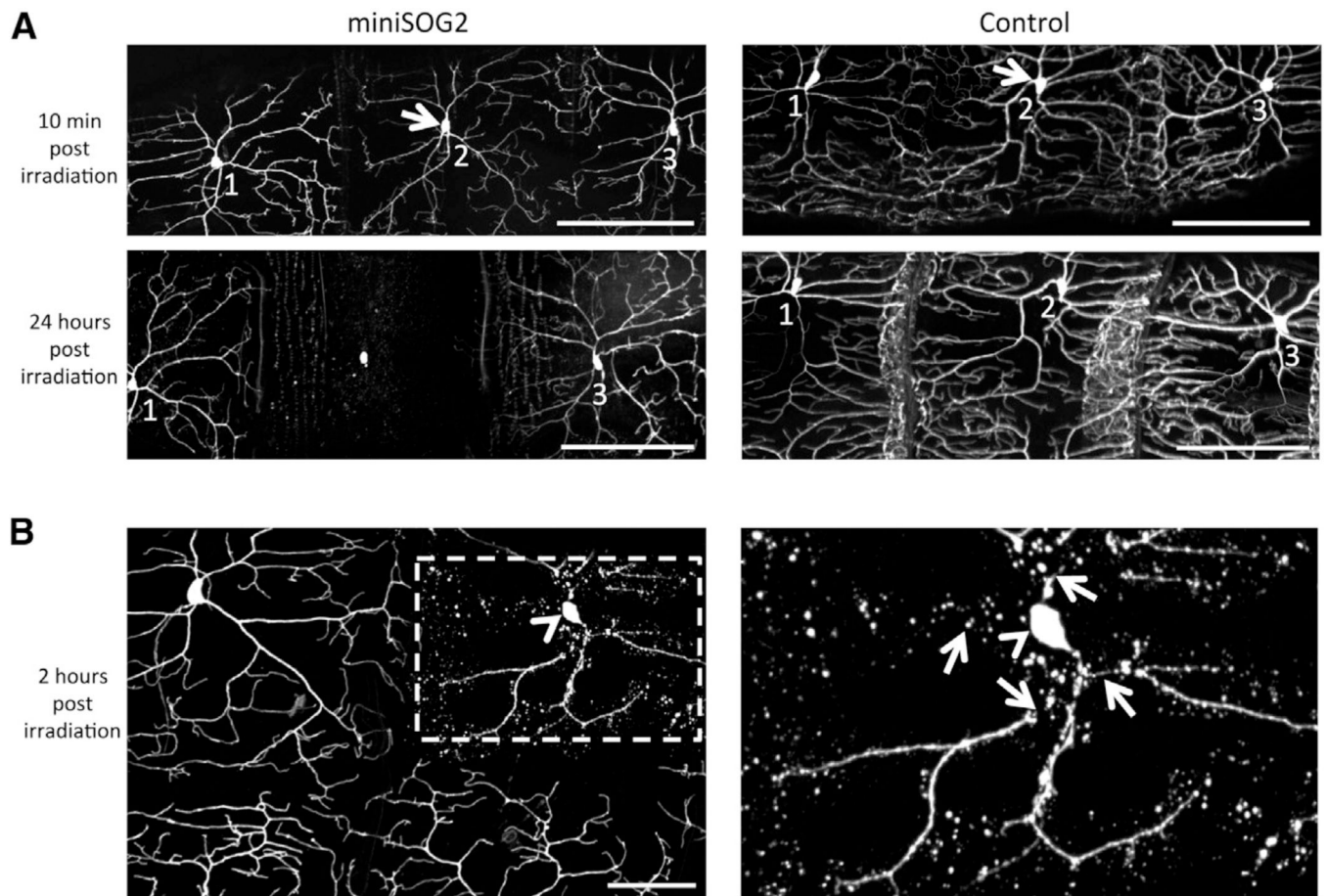Scale bars represent 100 μm.

Figure 3. Optogenetically Targeted Single-Neuron Ablation in *Drosophila*

(A) Fluorescence images of class IV da sensory neurons in *Drosophila* larvae. miniSOG2 was expressed in the class IV da sensory neurons (left panels). The neuronal processes were labeled by membrane-targeted (CD4) tdTomato. The control *Drosophila* only expressed CD4-tdTomato (right panels). Three neurons were imaged and neuron number 2 (arrows) was exposed to blue light. Upper and lower panels show orange fluorescence from tdTomato 10 min and 24 hr after blue-light illumination, respectively.

(B) Orange fluorescence images of class IV da sensory neurons in *Drosophila* 2 hr after blue-light illumination. The arrowhead points to the neuron exposed to blue light. The right panel shows a zoomed-in image of the boxed area in the left panel. The arrows point to fragmented and severed dendrites.

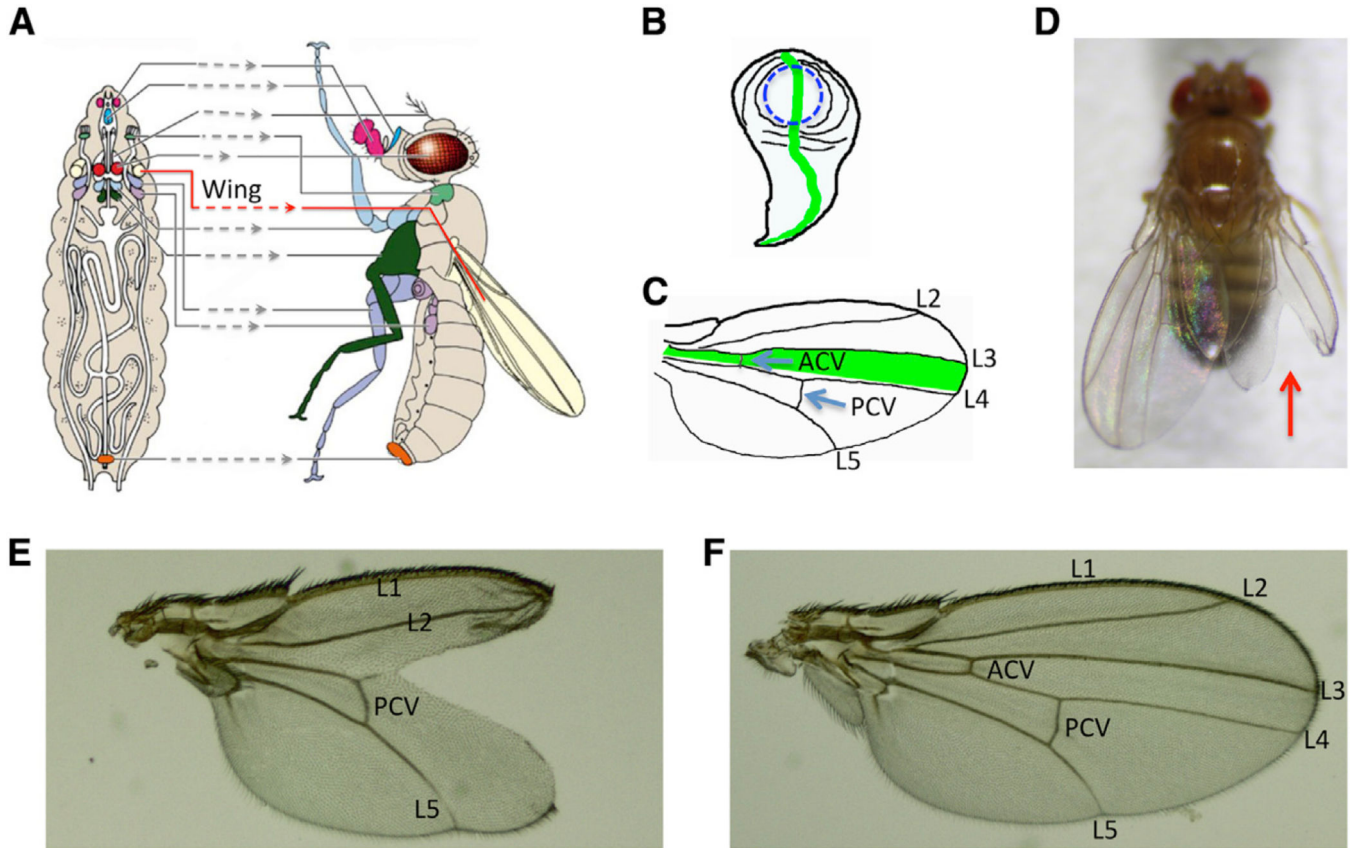Scale bars represent 150 μm (A), 50 μm (B).

Figure 4. Photoablation of *Dpp* Expressing Cells in *Drosophila* Wing

(A) Schematic of adult organs developed from larval imaginal discs, including the two wings (in yellow) from two wing imaginal discs (in yellow).

(B) Schematic of wing imaginal disc with *dpp*-expressing cells (in green). Blue-light illumination is restricted within the blue circle.

(C) Schematic of adult wing with *dpp*-expressing cells (in green).

(D) Adult fly developed from the optogenetically operated miniSOG2-expressing larva. The right wing loses a significant part of tissue (arrow) following photoablation of miniSOG2-expressing *dpp* cells in the wing imaginal disc as shown in (B). In contrast, the left wing that also expresses min-iSOG2 but is not exposed to blue light is normal.

(E) The right wing with significant tissue loss, including cells between L3 and L4, as well as ACV.

(F) The normal left wing. L1–L5: longitudinal veins. ACV, anterior cross vein; PCV, posterior cross vein.